

RESEARCH ARTICLE

Biomechanical determinants of bite force dimorphism in *Cyclommatus metallifer* stag beetles

Jana Goyens^{1,2,*}, Joris Dirckx², Manuel Dierick³, Luc Van Hoorebeke³ and Peter Aerts^{1,4}

ABSTRACT

In the stag beetle family (Lucanidae), males have diverged from females by sexual selection. The males fight each other for mating opportunities with their enlarged mandibles. It is known that owners of larger fighting apparatuses are favoured to win the male–male fights, but it was unclear whether male stag beetles also need to produce high bite forces while grabbing and lifting opponents in fights. We show that male *Cyclommatus metallifer* stag beetles bite three times as forcefully as females. This is not entirely unexpected given the spectacular nature of the fights, but all the more impressive given the difficulty of achieving this with their long mandibles (long levers). Our results suggest no increase in male intrinsic muscle strength to accomplish this. However, morphological analyses show that the long mandibular output levers in males are compensated by elongated input levers (and thus a wider anterior side of the head). The surplus of male bite force capability is realized by enlargement of the closer muscles of the mandibles, while overall muscle force direction remained optimal. To enable the forceful bites required to ensure male reproductive success, male head size and shape are adapted for long input levers and large muscles. Therefore, the entire head should be regarded as an integral part of male armature.

KEY WORDS: Lucanidae, Sexual dimorphism, Bite force, Functional morphology

INTRODUCTION

Insect mandibles are often adapted into tools for various tasks: e.g. fighting, digging, leaf-cutting, grooming and transporting liquids in ants; penetrating the soft tissues of snails and attaching to amphibian skin in ground beetles; cutting mature tree leaves and tearing and shredding young tree leaves in saturniids (Bernays, 1998; Bernays and Janzen, 1988; Ober et al., 2011; Paul, 2001; Wizen and Gasith, 2011). Male stag beetles (Lucanidae) are widely known for their extraordinary mandibles: a conspicuous sexual dimorphism where males can have mandibles in a variety of shapes that can be almost as long as their own body, while female mandibles are small and indistinct (Kawano, 2006). The small female mandibles are used to dig in rotten wood (for oviposition) and in soil (when emerging from their cocoon and to hide from predators), and possibly to pierce tree bark to feed from sap runs (Percy, 1998; Tanahashi et al., 2009; Tanahashi et al., 2010). Male stag beetles, however, fight each other with their enlarged mandibles to gain access to females (Emlen,

2008; Inoue and Hasegawa, 2013; Kawano, 2006; Shiokawa and Iwahashi, 2000; Tatsuta et al., 2001). During such fights, opponents try to grip each other and the winner will lift the other male and throw it backwards (Shiokawa and Iwahashi, 2000) (authors' personal observations; see supplementary material Movie 1). Male stag beetles with larger mandibles have been shown to win these male–male fights more often (Emlen et al., 2005; Hosoya and Araya, 2005; Tatsuta et al., 2001).

Most research on bite performance and sexual dimorphism has been performed on lizards. As in stag beetles, male lizards often have larger body and head sizes (Herrel et al., 1995; Herrel et al., 2007), the latter being correlated with higher male bite forces (Herrel et al., 1999; Herrel et al., 2001; Herrel et al., 2007; Verwaijen et al., 2002). It has been suggested that this sexual dimorphism arose by sexual selection on male bite force and natural selection on diet [prey size and toughness (Herrel et al., 1995; Herrel et al., 1999; Vanhooydonck et al., 2010)]. The large male stag beetle head may suggest a similar system, leading to higher bite force in males compared with females. However, it remains unexplored whether bite force, as such, determines fight outcome [such as already observed, for instance, in several lizard species, field crickets and fanged frogs (e.g. Emerson and Voris, 1992; Hall et al., 2010; Husak et al., 2006; Huyghe et al., 2005; Lailvaux et al., 2004)]. Indeed, fighting success in male stag beetles may rely equally well on firm interlocking between the ornamented jaws and the exoskeleton of the opponent without the need for a forceful pinch [comparable to the interlocking of antlers in fighting red deer stags (Clutton-Brock et al., 1979; Lincoln, 1972)]. If, however, forceful biting should prove to be important in stag beetle contests, male stag beetles face an additional problem: strongly elongated mandibles mean long output levers that reduce the force transmission from the closer muscles to the mandibular bite points. In this case, other compensatory adaptations for the enlarged output lever should be present in male stag beetles.

In this paper, we investigate the sexual dimorphism of the mandibular apparatus and the bite force in *Cyclommatus metallifer* Boisduval 1835 stag beetles. This Indonesian species belongs to the genus *Cyclommatus*, which includes (together with the genus *Prosopocoilus*) stag beetle species with the most oversized male mandibles (Gotoh et al., 2012; Kawano, 2006). In order to assess the effects of male sexual dimorphism on function and performance, one should, ideally, compare with non-dimorphic conspecific males. In (stag) beetles, comparison with properly scaled females (see Materials and methods) can be used as a proxy for such a hypothetical non-dimorphic male, as for species without sexual dimorphism (except for the reproductive organs), males and females can hardly (if at all) be discerned from each other (Hosoya and Araya, 2005; Kawano, 2006).

We hypothesize that males show an increased bite force performance compared with females. Okada and Hasegawa (Okada and Hasegawa, 2005) suggested that the stag beetle mating system is not based on female choice. Therefore, it seems likely that the

¹University of Antwerp, Laboratory of Functional Morphology, Universiteitsplein 1, B-2610 Antwerp, Belgium. ²University of Antwerp, Laboratory of BioMedical Physics, Groenenborgerlaan 171, B-2020 Antwerp, Belgium. ³Ghent University, UGCT-Department of Physics and Astronomy, Faculty of Sciences, Proeftuinstraat 86, 9000 Ghent, Belgium. ⁴Ghent University, Department of Movement and Sport Sciences, Watersportlaan 2, 9000 Ghent, Belgium.

*Author for correspondence (jana.goyens@uantwerpen.ac.be)

List of symbols and abbreviations

$F_{\text{bite,measured}}$	measured bite force, tangent to the orbit of the bite point
$F_{\text{bite,predicted}}$	calculated bite force
F_{muscle}	calculated muscle force
F_p	measured bite force, perpendicular to the bite plates
F_p	force perpendicular to the bite plates
MI	muscle insertion point on mandible
MMA	posterior body part, mesothorax + metathorax + abdomen
PCSA	physiological cross-sectional area
r_i	input lever vector
r_o	output lever vector
r_i	input lever length
r_o	output lever length
α	mandibular angle
β	3D angle between $F_{\text{bite,measured}}$ and r_o
γ	3D angle between F_{muscle} and r_i

mandibular system is optimized for fight performance. As mentioned, this should be accompanied by further adaptations of the mandibular system, e.g. as observed for the cheliceral system in camel spiders (van der Meijden et al., 2012). In this regard, the specific working hypotheses that we tested are: (1) males have prolonged input levers to compensate for their long output levers, (2) male mandibular muscles are geometrically advantageous compared with those of females (in terms of size and working direction), and (3) these muscles are intrinsically stronger than female muscles.

RESULTS

Bite performance and length tension relationship

Fig. 1 shows a representative example of the bite measurements, and illustrates the high repeatability of the bite tests. During the 30 s intervals, successive bursts of activity occur.

Maximal recorded bite force (over all mandible positions) is higher for males than for females (6.9 ± 2.0 and 1.1 ± 0.4 N, respectively). Normalized bite force (dimensionless) is also significantly higher for males than for females (849 ± 164 and 285 ± 81 , respectively; Wilcoxon rank sum test: $P < 0.001$).

To investigate the influence of muscle length on tension, male mandibular angles were converted into muscle lengths. Over the working range of mandible positions, a linear relationship between mandibular angle and muscle length exists: muscle length (mm) = $3.8 \text{ rad} + 7.1 \text{ mm}$ (linear regression: $P < 0.001$).

Fig. 2 shows the relationship between muscle length (obtained with the above equation) and maximal bite force. A negative relationship between force and muscle length exists: males produce the highest forces with their mandibles almost closed (see Fig. 2). Video analysis of male–male fights shows that they bite most frequently with 4.1 ± 2.0 mm between their bite points. Within the corresponding range of normalized muscle lengths, the highest bite forces are measured (see Fig. 2, shaded area).

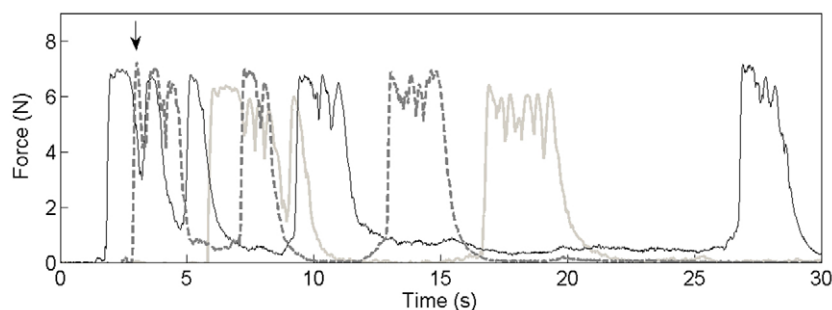


Fig. 1. Example of force measurements in *Cyclommatus metallifer*. Three trails from the same male individual, obtained at a bite plate distance of 5 mm. The arrow indicates the overall maximum of 7.22 N.

Morphology and morphometrics

Micro-CT reconstructions give us an insight into the interior of the head (see Fig. 3). The general anatomy of the head is similar to that of other beetles (Gorb and Beutel, 2000; Li et al., 2011). The mandibles articulate by a hinge axis, formed by a pair of condyles. The closer muscle is cone shaped and is distinctly larger than the opener muscle: it almost completely fills the head capsule.

Table 1 provides the input and output lever lengths as well as the lever ratios. In absolute terms, as well as expressed relative to the width of the posterior part of the body [mesothorax + metathorax + abdomen (MMA); see Fig. 5], the males have longer levers than the females. The lever ratio is not significantly different between males and females, as shown by the nonparametric Wilcoxon rank sum test ($P = 0.051$). Given the low P -value and the low statistical power of the test, this indicates that the long input levers compensate for the long male output levers, albeit probably not completely.

Muscle geometry

Male as well as female mandible closer muscles almost fill the entire head (see Morphology and morphometrics, above). However, because head shape and relative size differ, the normalized physiological cross-sectional area (PCSA) of the male closer muscle is almost 2.5 times larger (see Table 1).

The force components of the closer muscle in the x -, y - and z -directions are given in Table 2, averaged over the range of *in vivo* used mandible positions (see Fig. 4). The absolute value of the y -component lies very close to 1 for both males and females, indicating that the muscle force vector is well aligned with the y -axis, which is the optimal direction. This holds true in the entire working range of mandible position (i.e. small standard deviation).

Comparison of measured and predicted bite forces

The theoretical ratio of male and female bite force can be predicted (according to Eqn 3) using the geometrical properties of the two CT-scanned individuals. The weight-normalized values of PCSA are used:

$$\frac{|F_{\text{bite,predicted,male}}|}{|F_{\text{bite,predicted,female}}|} = \frac{6220}{2557} \times \frac{0.96}{0.95} \times \frac{0.28}{0.34} = 2.03. \quad (1)$$

This is close to the ratio of maximal measured bite force for these two individuals (also normalized to MMA weight):

$$\frac{|F_{\text{bite,measured,male}}|}{|F_{\text{bite,measured,female}}|} = \frac{7.9}{3.9} = 2.06. \quad (2)$$

Muscle stress

We measured maximal bite forces of 6.5 and 1.6 N for the male and female individuals, respectively, that were used for micro-CT scanning. This corresponds to (maximal) muscles forces of 9.9 and

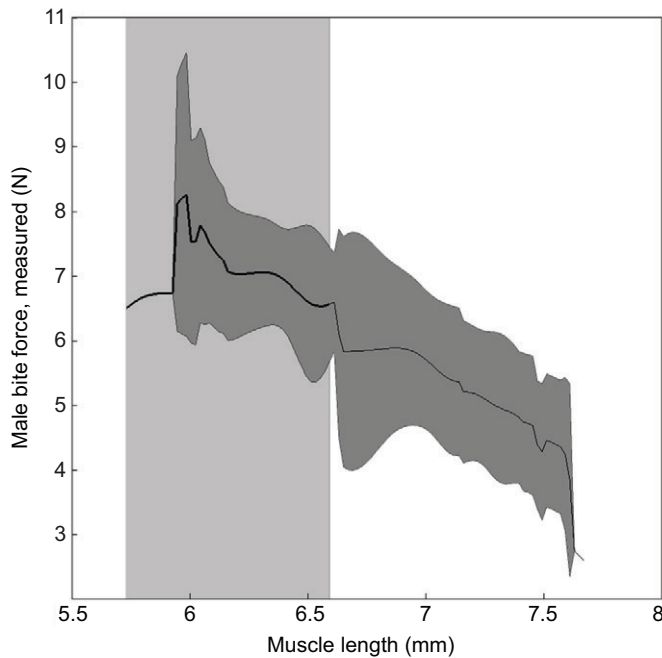


Fig. 2. Male bite force as a function of muscle length. Mean \pm s.d. of nine specimens are shown. The shaded area indicates the range of most frequently used muscle lengths in fights (with 4.1 ± 2.0 mm biting point distance).

2.4 N. Divided by attachment area, this gives almost equal (maximal) muscle stresses of 18 N cm^{-2} for the male and 17 N cm^{-2} for the female specimen.

DISCUSSION

Similar to how red deer stags grow large antlers to defend harems of females, male stag beetles bear heavy and long mandibles to fight for mating opportunities (Emlen et al., 2005; Inoue and Hasegawa, 2013; Kawano, 2006; Kruuk et al., 2002; Shiokawa and Iwahashi, 2000; Tatsuta et al., 2001). The longer the mandibles, the higher the chances of winning (Emlen et al., 2005; Tatsuta et al., 2001). The same was observed for male dung beetles, who try to probe and dislodge intruder males with their horns in narrow burrows (Emlen, 2008). It is likely that both stag beetles and dung beetles take advantage of longer mandibles or horns by extending their reach towards opponents. However, this mandibular elongation could come at a cost if high bite forces are required, because of a disadvantageously long output lever. Because our study species, *C. metallifer*, belongs to one of the genera with the relatively longest male mandibles (Gotoh et al., 2012; Kawano, 2006), it is most prone to a reduced force output. Therefore, we expect distinct adaptations if high bite forces are generated.

Table 1. Absolute and normalized values of lever length, lever ratio and physiological cross-sectional area (PCSA) of the closer muscle in the stag beetle *Cyclommatus metallifer*

	Absolute value		Normalized value (dimensionless)	
	Male	Female	Male	Female
Input lever length (mm)	3.4 ± 0.4	1.0 ± 0.12	36.8 ± 2.6	14.0 ± 1.7
Output lever length (mm)	12.9 ± 3.2	3.1 ± 0.20	140.6 ± 1	41.7 ± 2.8
Lever ratio	0.28 ± 0.07	0.34 ± 0.04		
PCSA (mm^2)	54.71	13.95	6220	2557

Lever lengths are normalized to $\text{MMA mass}^{1/3}$ and PCSA to $\text{MMA mass}^{2/3}$, where MMA is the mesothorax + metathorax + abdomen. The lever lengths and lever ratios are averaged for nine males and 10 females; data are means \pm s.d.

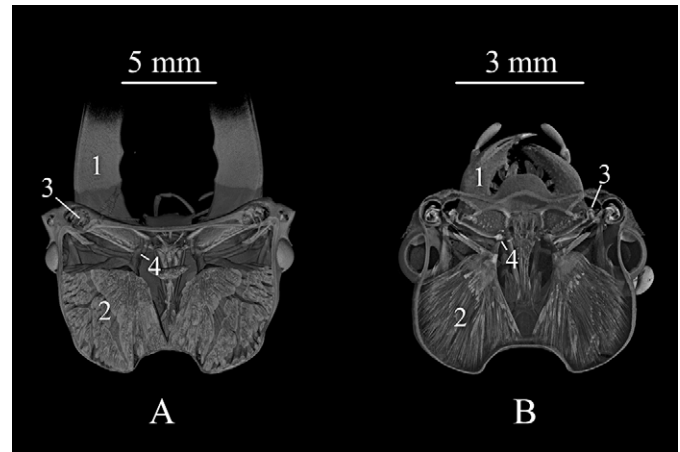


Fig. 3. Micro-CT renderings of *Cyclommatus metallifer* stag beetle heads. For a male (A) and a female (B) specimen, a mandible (1), cone shaped mandible closer muscle (2), condyle of mandible rotation hinge (3) and muscle insertion on the mandible (4) are indicated.

Our bite force measurements show that male *C. metallifer* individuals indeed bite more forcefully than female specimens. Even when normalized to size, a threefold intersexual difference in maximal bite force exists. So males have, indeed, stepped up their bite force performance, which indicates that forceful biting is important for male beetles. This is further supported by the finding that males use their mandible muscles during fights at optimal or close to optimal fiber lengths (see Fig. 2). As with lizards, they probably need the increased bite force in the first place for male–male combat. Males may also benefit from high bite forces during the mating itself, by preventing females from escaping. The same has also been suggested for lizards (Herrel et al., 1995). In lizards, sexual bite force dimorphism is known to be caused by natural selection as well, through selection for niche divergence to lower intersexual competition (Herrel et al., 1995; Vanhooydonck et al., 2010). This is most probably not the case for stag beetles, because males do not use their mandibles for feeding (Tanahashi et al., 2009; Tanahashi et al., 2010). Interestingly, the muscle force males exert depends on the used bite point: males use less muscle force when biting at the very tips of the mandibles (J.G., J. Soons, P.A. and J.D., unpublished data). Whether this has a behavioral or a mechanical (material failure) cause will be the subject of future research.

To investigate the adaptations enabling such high bite forces, we micro-CT-scanned a specimen of each sex. The bite force ratio of these individuals equals 2.06. When we calculate the same ratio using geometrical data, we arrive at an almost identical value of 2.03. As it seems very unlikely that both sexes perform at the same relative submaximal level in the *in vivo* experiments, we assume that

Table 2. x-, y- and z-components of the global force direction of the closer muscle of the mandible of one male and one female *Cyclommatus metallifer*

	Male	Female
x-component	0.27±0.04	0.28±0.14
y-component	0.96±0.01	0.95±0.05
z-component	0.21±0.02	0.09±0.02

Means and standard deviations over the range of possible mandible positions are given.

the *in vivo* performance reflects maximal performance. Also, the estimates for maximal muscle stress in males and females are almost identical (18 and 17 N cm⁻², respectively) and lie well within the range of calculated and measured stresses of (synchronous) insect muscle (2 to 80 N cm⁻²) (Bennet-Clark, 1975; Ellington, 1985; Full and Ahn, 1995; Usherwood, 1962; Wheeler and Evans, 1989). All of these arguments not only support the followed procedure to estimate PCSA, but also suggest that there is no intersexual difference in the physiology of the jaw closers of stag beetles, and that the characteristics of these closer muscles are not specialized compared with other (synchronous) insect muscles. Hence, other factors are required to explain the size-normalized male/female ratio in biting force.

The accordance of measured and geometrically predicted force ratios shows that sexual selection altered the geometry and dimensions of not only the male mandibles, but also the entire male head. First, the length of the input levers has increased to compensate for the elongated output levers, keeping the lever ratio close to that of females. Functional adaptations of the input lever have previously been observed for other beetle species: larvae of detritus-grinding and snail-cracking species were shown to have larger input levers than larvae of a liquid-feeding species (Gorb and Beutel, 2000). And in camel spider chelicerae, the lever system is adapted to their function (digging in compact soil versus crushing hard prey) (van der Meijden et al., 2012). Second, males have larger closer muscles than females. The morphology of the posterior part of the insect head capsule (where the closer muscles attach) is known to be closely related to (or even ontologically caused by) the

size and shape of the mandible closer muscle (Gorb and Beutel, 2000; Li et al., 2011; Paul, 2001). Our observations of broad male stag beetle heads led us to hypothesize that males have relatively larger muscles than females. PCSA calculations confirm this: male attachment surfaces are more than twice as large as those of females, theoretically enabling more than twice as much force production. This is comparable to the finding of enlarged jaw adductor musculature in *Anolis* and *Podarcis* lizards, causing elevated bite force performance (Herrel et al., 1995; Herrel et al., 2007; Huyghe et al., 2009). Despite the hypertrophy of the male stag beetle adductor muscles, they remain well aligned with the optimal direction. This indicates that the male head shape changed in such a way that the same percentage of the total muscle force remained useful.

In order to reproduce, a male stag beetle needs large mandibles and forceful bites. We showed that no physiological adaptations of the mandible closer muscles are necessary to arrive at the observed intersexual bite force dimorphism. The large and well-aligned male muscles combined with increased input levers to compensate for the elongated output levers offer a sufficient explanation. This, however, required substantial geometrical differentiation of the male head. Therefore, the entire male stag beetle head (and not only the male mandibles) should be seen as part of male weaponry, as suggested by Shiokawa and Iwahashi (Shiokawa and Iwahashi, 2000). When assessing the effects of this sexual dimorphism on other important ecological functions (such as locomotion), head size and morphology might become even more important than jaw size and morphology.

MATERIALS AND METHODS

Animals

Adult *C. metallifer* individuals were obtained from a commercial dealer (Kingdom of Beetle, Taipei, Taiwan). The animals were individually housed in plastic containers (39×28×14 cm, length × width × height), at a temperature of between 20 and 25°C. They were fed beetle jelly and water *ad libitum*.

Bite force measurements

Bite forces were obtained from nine male (1.36±0.28 g) and 10 female (0.55±0.10 g) beetles with an isometric Kistler force transducer (type 9203, Kistler Inc., Winterthur, Switzerland) connected to a Kistler charge amplifier (type 5058A). The force transducer was mounted in a setup with two small plates that were grasped by the mandibles, thus enabling us to measure bite forces. Spacing between the bite plates could be adjusted [for a detailed description of the experimental setup, see Herrel et al. (Herrel et al., 1999)]. The analog signals were A/D converted (USB-6009, 14-bit, National Instruments, Austin, TX, USA) and recorded at a sample frequency of 200 Hz using a purpose-written LabVIEW routine (LabVIEW 9.0.1f2, 32-bit version, National Instruments). When a defensive response was provoked, males bit the bite plates with the large protrusions positioned halfway along the mandibles (P; see Fig. 5). In real fights, males also regularly (but not exclusively) use the mandibular protrusions. These were selected as the experimental bite point because: (1) they provide point contact with the bite plates, (2) they guarantee standardized experimental conditions within and between individuals (i.e. similar location of force application) and (3) males were eager to bite with them. Females bit with the tip of their mandibles, the only possibility given their jaw size and morphology. The minimal distance between the bite plates (imposed by the constraints of the setup) was 3 mm for both sexes. The maximal possible bite plate distance (behaviorally imposed: when the spacing became too large, specimens refused to bite) was 5 mm for females and 12 mm for males. We varied the distance between the bite plates between these boundaries with intervals of 1 mm. The sequence was determined randomly. For every plate distance (and hence mandibular angle) three recordings of 30 s were made, and the highest force observed in these 90 s recording was retained as the maximal bite force for that individual.

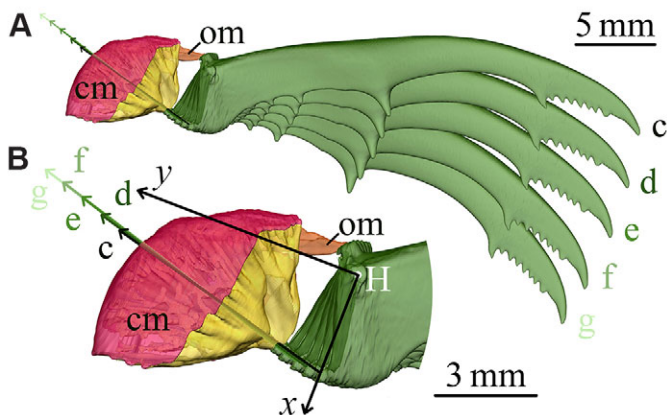


Fig. 4. Micro-CT segmentations of male *Cyclommatus metallifer* stag beetle mandibles. (A) Male mandible and the associated closer (cm) and opener muscles (om). The mandible is shown in the CT-scanned position (g) and with 3, 6, 9 and 12 mm between the bite points (f, e, d and c). The muscle force vectors associated with these mandible positions are also shown. (B) Enlargement of A, with designation of the muscle force vectors. The x- and y-axes are shown for mandible position c. The location of the rotation hinge (H) is the same for all mandible positions.

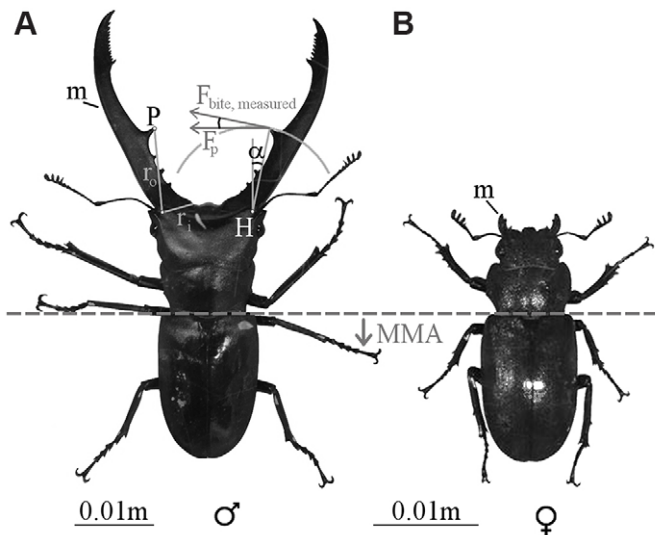


Fig. 5. Dorsal photographs of *Cyclommatus metallifer* stag beetles. For a male (A) and female (B) individual, one mandible is marked (m). Body parts below the dashed line are the mesothorax, metathorax and abdomen (MMA). Note that the images are scaled to identical MMA length. For the male, a bite point (P), input and output levers (r_i and r_o), mandibular angle (α) as well as the position of the rotation hinge (H) are indicated. The measured bite force (F_p , perpendicular to the bite plates) and the actual exerted bite force ($F_{\text{bite,measured}}$, tangential to the orbit of the bite point) are also shown.

The degree of mandibular abduction (imposed by the bite plate spacing) was taken into account, as effects of muscle length according to the length–tension relationships could be expected. We defined the mandibular angle as the angle between the long axis of the body and the line from the rotation axis of the mandible to the bite point (α , see Fig. 5). This angle was determined on high-resolution digital photographs using GIMP (GNU Image Manipulation Program 2.6.11; open source software; average precision males: $30 \mu\text{m pixel}^{-1}$; average precision females: $20 \mu\text{m pixel}^{-1}$). The force transducer only measures force components perpendicular to the bite plates (F_p ; see Fig. 5). The real bite force, tangent to the orbit of the biting point ($F_{\text{bite,measured}}$, see Fig. 5), was derived by dividing F_p by the cosine of the mandibular angle α . For male–female comparisons, normalization was necessary because of the large size difference between the sexes. Given the strong sexual dimorphism of the anterior part of the body, bite forces were normalized to the weight (in N) of the posterior part of the body (MMA), the size of which can safely be assumed to be entirely independent of the mandibular apparatus. The MMA was weighed with an analytical microbalance (Mettler Toledo MT5, Greifensee, Switzerland; precision: $1 \mu\text{g}$) after killing the specimens.

Levers

Male and female mandible morphology differ greatly. To enable intersexual bite force comparison, the lever mechanics have to be taken into account. The lengths of the input lever (r_i , between the mandibular hinge joint and the muscle insertion point on the mandible MI; see Figs 3, 5) and output lever (r_o , between the mandibular hinge joint and the biting point; see Fig. 5) were measured from scaled photographs in GIMP. To enable male–female comparison of the levers, they were normalized to MMA mass (used as proxy for MMA volume; i.e. identical overall MMA densities are assumed), raised to the power of $1/3$. Lever ratios (mechanical advantage; input lever divided by output lever) were also calculated.

Micro-CT scans and segmentation

The anterior portion (head + prothorax) of each specimen was fixed in Bouin's solution (Sigma-Aldrich, St Louis, MO, USA) for 2 weeks. Then, they were brought to 100% ethanol (in steps of 70, 80, 90 and 96% ethanol) and subsequently stained in a 1% iodine solution (I_2 dissolved in 100%

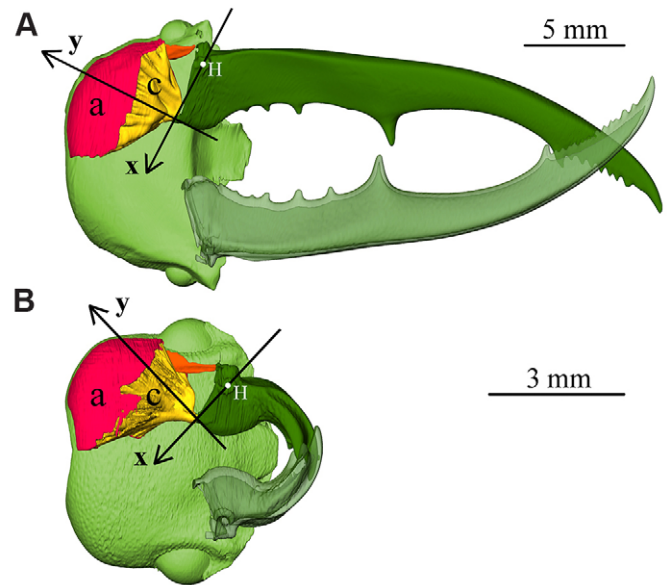


Fig. 6. Micro-CT segmentations of *Cyclommatus metallifer* stag beetle heads. For a male (A) and female (B) head, the left mandible, the closer muscle (c) and its attachment surface (a) are shown, as well as the rotation hinge (H) and the x- and y-axes used to calculate the direction of the total muscle force vector. A part of the associated opener muscle is also visible (orange). The right mandible is depicted transparently.

ethanol; Sigma-Aldrich) for 20 days (adapted from Metscher, 2009). Finally, the samples were thoroughly washed with and stored in 100% ethanol.

One male and one female specimen were removed from alcohol and mounted in a falcon tube with cotton wool for micro-CT scanning. A custom built X-ray micro-CT scanner of medium energy from UGCT, the Centre for X-ray Tomography of Ghent University, was used (Masschaele et al., 2007). For the male sample, the X-ray source was operated at 130 kV and $107.7 \mu\text{A}$, for the female sample 120 kV and $116.7 \mu\text{A}$ were used, both with an aluminum filter of 1 mm thickness. For both samples, 1200 projections with an exposure time of 2 s each were recorded over 360 deg. The section images were reconstructed with the custom-made software package Octopus (Vlassenbroeck et al., 2007). This resulted in reconstructed images of 790×805 pixels for the male specimen and 760×750 pixels for the female specimen, and voxel sizes of 38 and $13 \mu\text{m}$, respectively. Three-dimensional renderings were generated using the commercial package VGStudioMAX (Volume Graphics, Heidelberg, Germany). Unless otherwise specified, all further calculations were performed only for these two specimens.

Using the reconstructed slice images, one mandible and the associated closer (adductor) muscle (craniomandibularis internus; see Fig. 6) of each sample were segmented in Amira (Amira 5.4.3; 64-bit version; VSG systems, Mérégnac, France). The attachment surface (see Fig. 6) of the closer muscle at the posterior side of the head was segmented separately, and a smooth surface model was created.

Muscle size, force direction and muscle stress

The muscle fibers converge from the convex (nearly spherical, see Fig. 6) head capsule to the MI (see Fig. 3). Therefore, the size of the attachment surface (see Fig. 6) can be used as a proxy for the PCSA of the muscle and hence of force production. To assess the area of the attachment surface, its surface model was converted into a triangulated surface mesh in Geomagic (Geomagic 10, Morrisville, NY, USA; male specimen: 4894 triangles; female specimen: 5322 triangles). In MATLAB (MATLAB R2012a, 7.14.0.739, 64-bit version; Natick, MA, USA), we calculated the area of each triangle using the 3D coordinates of its vertices, to obtain the total area of the attachment surface in males as well as females. This area was normalized to MMA mass, raised to the power of $2/3$.

For optimal force transmission towards the output lever, the combined force of all muscle fibers of the closer muscle should be directed perpendicular to the rotation axis and the input lever (along the y -axis in Fig. 6; x aligned with the input lever, z points downwards, following the rotation axis, and $y=z \times x$). Muscle force components in the x - or z -direction have no influence on force output at the biting point, but they do induce stress on the hinge joint suspension and can, therefore, be expected to be minimized. We estimated the global muscle force direction by summing the unit vectors from the MI to every vertex of the triangular mesh of the attachment surface. The total muscle force vector was divided by its norm to create a unit vector. This calculation was repeated for the other MI positions that correspond to the different mandibular abduction angles, covering the range of mandible positions in the experiments and CT scans (male: 0.8 to 12 mm between biting points in steps of 1 mm for males; -1.5 to 5 mm in steps of 0.5 mm for females; see Fig. 4).

Using only these geometrical data (muscle attachment area, 3D orientation of the hinge and lever lengths), it is possible to predict male to female bite force ratio:

$$\frac{|\mathbf{F}_{\text{bite,predicted,male}}|}{|\mathbf{F}_{\text{bite,predicted,female}}|} = \frac{\text{PCSA}_{\text{male}}}{\text{PCSA}_{\text{female}}} \times \frac{y_{\text{male}}}{y_{\text{female}}} \times \frac{R_{\text{male}}}{R_{\text{female}}}, \quad (3)$$

where y_{male} and y_{female} are the y -component muscle force unit vectors for male and females, respectively, and R_{male} and R_{female} are the male and female lever ratios, respectively.

Besides geometrical differences, male muscle stress could also be enhanced in order to increase bite performance. Muscle stress is defined as the muscle force per cross-sectional area of a muscle. Muscle force $\mathbf{F}_{\text{muscle}}$ was obtained from the moment balance:

$$\mathbf{F}_{\text{muscle}} \times \mathbf{r}_i = \frac{1}{2} \mathbf{F}_{\text{bite,measured}} \times \mathbf{r}_o, \quad (4)$$

$$|\mathbf{F}_{\text{muscle}}| = \frac{1}{2} |\mathbf{F}_{\text{bite,measured}}| \cdot |\mathbf{r}_o| \cdot \sin(\beta) / [|\mathbf{r}_i| \cdot \sin(\gamma)], \quad (5)$$

where \mathbf{r}_i and \mathbf{r}_o are the 3D input and output lever vectors, $\frac{1}{2} \mathbf{F}_{\text{bite,measured}}$ is the maximal bite force of one mandible of the scanned individuals, and β and γ are the 3D angles between the force vectors and their respective levers, calculated from 3D coordinates on the surface model. Assuming that animals make an effort to bite maximally, the calculated muscle stress ($\mathbf{F}_{\text{muscle}}/\text{PCSA}$) represents maximal (isometric) stress.

Length-tension relationship

Because force output is influenced by muscle length (Gordon et al., 1966), we wanted to convert the range of mandibular angles in the male biting experiments into muscle lengths. Knowing the total muscle force vector enabled us to calculate the distance between the MI and the point at which the resultant force vector crosses the attachment surface. This gives the length of an imaginary muscle fiber with the direction of the global force vector that could replace the real closer muscle. We repeated this for the same range of MI positions as for the force direction calculation (see Fig. 4). The resulting relationship between mandibular angle and muscle length was used to convert the mandibular angles of all nine males in the biting experiments into muscle lengths. This enabled us to plot the force measurements in function of muscle length. Given the limited range of gaping angles for the females (see above, three bite widths only), their length-tension relationship could not be determined.

To determine the most frequently used muscle lengths, high-speed recordings were made of fighting males (combinations of all nine males). Two beetles were placed in an open-top arena (15×15 cm), with a base covered with smooth cork for grip. Four mirrors functioned as walls and were placed at an angle of 45 deg, so five views could be recorded with one camera (Redlake HR1000; 125 frames s⁻¹). Twenty-three recordings of males who bit an opponent were obtained.

In each of these recordings, the distance between the medial mandibular protrusions (the biting points in the force measurements) relative to the distance between the eyes was determined in GIMP. Absolute distances between the eyes were measured on scaled digital photographs of the beetles, which enabled us to infer the absolute distance between the medial

mandibular protrusions. These distances were converted into mandibular angles and subsequently into muscle lengths.

Acknowledgements

We thank Dr Kristiaan D'Août for writing the LabVIEW routine for recording the force measurements and Josie Meaney for proofreading an earlier version of the manuscript.

Competing interests

The authors declare no competing financial interests.

Author contributions

J.G. conducted the bite experiments, segmented the micro-CT scans and drafted the article. J.G., P.A. and J.D. were involved in the analyses and interpretation of the findings and revised the article. M.D. and L.V.H. executed the micro-CT scans, CT reconstruction and 3D renderings.

Funding

The present study was funded by BOF grant [ID BOF UA 2011-445-a] of the Research Council of University of Antwerp.

Supplementary material

Supplementary material available online at

<http://jeb.biologists.org/lookup/suppl/doi:10.1242/jeb.091744/-/DC1>

References

- Bennet-Clark, H. C. (1975). The energetics of the jump of the locust *Schistocerca gregaria*. *J. Exp. Biol.* **63**, 53-83.
- Bernays, E. A. (1998). Evolution of feeding behavior in insect herbivores. Success seen as different ways to eat without being eaten. *Bioscience* **48**, 35-44.
- Bernays, E. A. and Janzen, D. H. (1988). Saturniid and sphingid caterpillars: two ways to eat leaves. *Ecology* **69**, 1153-1160.
- Clutton-Brock, T., Albon, S. D., Gibson, R. M. and Guinness, F. E. (1979). The logical stag: adaptive aspects of fighting in red deer (*Cervus elaphus* L.). *Anim. Behav.* **27**, 211-225.
- Ellington, C. P. (1985). Power and efficiency of insect flight muscle. *J. Exp. Biol.* **115**, 293-304.
- Emerson, S. B. and Voris, H. (1992). Competing explanations for sexual dimorphism in a voiceless Bornean frog. *Funct. Ecol.* **6**, 654-660.
- Emlen, D. J. (2008). The evolution of animal weapons. *Annu. Rev. Ecol. Evol. Syst.* **39**, 387-413.
- Emlen, D. J., Marangelo, J., Ball, B. and Cunningham, C. W. (2005). Diversity in the weapons of sexual selection: horn evolution in the beetle genus *Onthophagus* (Coleoptera: Scarabaeidae). *Evolution* **59**, 1060-1084.
- Full, R. and Ahn, A. (1995). Static forces and moments generated in the insect leg: comparison of a three-dimensional musculo-skeletal computer model with experimental measurements. *J. Exp. Biol.* **198**, 1285-1298.
- Gorb, S. and Beutel, R. G. (2000). Head-capsule design and mandible control in beetle larvae: a three-dimensional approach. *J. Morphol.* **244**, 1-14.
- Gordon, A. M., Huxley, A. F. and Julian, F. J. (1966). The variation in isometric tension with sarcomere length in vertebrate muscle fibres. *J. Physiol.* **184**, 170-192.
- Gotoh, H., Fukaya, K. and Miura, T. (2012). Heritability of male mandible length in the stag beetle *Cyclommatus metallifer*. *Entomol. Sci.* **15**, 430-433.
- Hall, M. D., McLaren, L., Brooks, R. C. and Lailvaux, S. P. (2010). Interactions among performance capacities predict male combat outcomes in the field cricket. *Funct. Ecol.* **24**, 159-164.
- Herrel, A., Van Damme, R. and De Vree, F. (1995). Sexual dimorphism of head size in *Podarcis hispanica atrata*: testing the dietary divergence hypothesis by bite force analysis. *Neth. J. Zool.* **46**, 253-262.
- Herrel, A., Spithoven, L., Van Damme, R. and De Vree, F. (1999). Sexual dimorphism of head size in *Gallotia galloti*: testing the niche divergence hypothesis by functional analyses. *Funct. Ecol.* **13**, 289-297.
- Herrel, A., De Grauw, E. and Lemos-Espinal, J. A. (2001). Head shape and bite performance in xenosaurid lizards. *J. Exp. Zool.* **290**, 101-107.
- Herrel, A., McBrayer, L. D. and Larson, P. M. (2007). Functional basis for sexual differences in bite force in the lizard *Anolis carolinensis*. *Biol. J. Linn. Soc. Lond.* **91**, 111-119.
- Hosoya, T. and Araya, K. (2005). Phylogeny of Japanese stag beetles (Coleoptera: Lucanidae) inferred from 16S mtDNA gene sequences, with reference to the evolution of sexual dimorphism of mandibles. *Zool. Sci.* **22**, 1305-1318.
- Husak, J. F., Lappin, K. A., Fox, S. F. and Lemos-Espinal, J. A. (2006). Bite-force performance predicts dominance in male venerable collared lizards (*Crotaphytus antiquus*). *Copeia* **2006**, 301-306.
- Huyghe, K., Vanhooydonck, B., Scheers, H., Molina-Borja, M. and Van Damme, R. (2005). Morphology, performance and fighting capacity in male lizards, *Gallotia galloti*. *Funct. Ecol.* **19**, 800-807.
- Huyghe, K., Herrel, A., Adriaens, D., Tadić, Z. and Van Damme, R. (2009). It is all in the head: morphological basis for differences in bite force among colour morphs of the Dalmatian wall lizard. *Biol. J. Linn. Soc. Lond.* **96**, 13-22.

- Inoue, A. and Hasegawa, E. (2013). Effect of morph types, body size and prior residence on food-site holding by males of the male-dimorphic stag beetle *Prosopocoilus inclinatus* (Coleoptera: Lucanidae). *J. Ethol.* **31**, 55-60.
- Kawano, K. (2006). Sexual dimorphism and the making of oversized male characters in beetles (Coleoptera). *Ann. Biomed. Eng.* **99**, 327-341.
- Kruuk, E. B., Slate, J., Pemberton, J. M., Brotherstone, S., Guinness, F. and Clutton-Brock, T. (2002). Antler size in red deer: heritability and selection but no evolution. *Evolution* **56**, 1683-1695.
- Lailvaux, S. P., Herrel, A., Vanhooydonck, B., Meyers, J. J. and Irschick, D. J. (2004). Performance capacity, fighting tactics and the evolution of life-stage male morphs in the green anole lizard (*Anolis carolinensis*). *Proc. R. Soc. B* **271**, 2501-2508.
- Li, D., Zhang, K., Zhu, P., Wu, Z. and Zhou, H. (2011). 3D configuration of mandibles and controlling muscles in rove beetles based on micro-CT technique. *Anal. Bioanal. Chem.* **401**, 817-825.
- Lincoln, G. A. (1972). The role of antlers in the behaviour of red deer. *J. Exp. Zool.* **182**, 233-249.
- Masschaele, B. C., Cnudde, V., Dierick, M., Jacobs, P., Van Hoorebeke, L. and Vlassenbroeck, J. (2007). UGCT: new X-ray radiography and tomography facility. *Nucl. Instrum. Methods* **580A**, 266-269.
- Metscher, B. D. (2009). MicroCT for comparative morphology: simple staining methods allow high-contrast 3D imaging of diverse non-mineralized animal tissues. *BMC Physiol.* **9**, 11.
- Ober, K., Matthews, B., Ferrieri, A. and Kuhn, S. (2011). The evolution and age of populations of *Scaphinotus petersi* Roeschke on Arizona Sky Islands (Coleoptera, Carabidae, Cychrini). *ZooKeys* **197**, 183-197.
- Okada, Y. and Hasegawa, E. (2005). Size-dependent precopulatory behavior as mate-securing tactic in the Japanese stag beetle, *Prosopocoilus inclinatus* (Coleoptera; Lucanidae). *J. Ethol.* **23**, 99-102.
- Paul, J. (2001). Mandible movements in ants. *Comp. Biochem. Physiol.* **131A**, 7-20.
- Percy, C. (1998). *Findings of the 1998 National Stag Beetle Survey*. London: Mammal Trust UK; People's Trust for Endangered Species.
- Shiokawa, T. and Iwahashi, O. (2000). Mandible dimorphism in males of a stag beetle, *Prosopocoilus dissimilis okinawanus* (Coleoptera: Lucanidae). *Appl. Entomol. Zool.* **35**, 487-494.
- Tanahashi, M., Matsushita, N. and Togashi, K. (2009). Are stag beetles fungivorous? *J. Insect Physiol.* **55**, 983-988.
- Tanahashi, M., Kubota, K., Matsushita, N. and Togashi, K. (2010). Discovery of mycangia and the associated xylose-fermenting yeasts in stag beetles (Coleoptera: Lucanidae). *Naturwissenschaften* **97**, 311-317.
- Tatsuta, H., Mizota, K. and Akimoto, S. (2001). Allometric patterns of heads and genitalia in the stag beetle *Lucanus maculifemoratus* (Coleoptera: Lucanidae). *Ann. Entomol. Soc. Am.* **94**, 462-466.
- Usherwood, P. N. R. (1962). The nature of "slow" and "fast" contractions in the coxal muscles of the cockroach. *J. Insect Physiol.* **8**, 31-52.
- van der Meijden, A., Langer, F., Boistel, R., Vagovic, P. and Heethoff, M. (2012). Functional morphology and bite performance of raptorial chelicerae of camel spiders (Solifugae). *J. Exp. Biol.* **215**, 3411-3418.
- Vanhooydonck, B., Cruz, F. B., Abdala, C. S., Azócar, D. L. M., Bonino, M. F. and Herrel, A. (2010). Sex-specific evolution of bite performance in *Liolaemus* lizards (Iguania: Liolaemidae): the battle of the sexes. *Biol. J. Linn. Soc. Lond.* **101**, 461-475.
- Verwajen, D., Van Damme, R. and Herrel, A. (2002). Relationships between head size, bite force, prey handling efficiency and diet in two sympatric lacertid lizards. *Funct. Ecol.* **16**, 842-850.
- Vlassenbroeck, J., Dierick, M., Masschaele, B., Cnudde, V., Van Hoorebeke, L. and Jacobs, P. (2007). Software tools for quantification of X-ray microtomography at the UGCT. *Nucl. Instrum. Methods* **580A**, 442-445.
- Wheater, C. P. and Evans, M. E. G. (1989). The mandibular forces and pressures of some predacious Coleoptera. *J. Insect Physiol.* **35**, 815-820.
- Wizen, G. and Gasith, A. (2011). An unprecedented role reversal: ground beetle larvae (Coleoptera: Carabidae) lure amphibians and prey upon them. *PLoS ONE* **6**, e25161.